Supplementary Information for:

Commercial photocatalyst changes the behavior of *Formica pratensis* and *Formica polyctena*

Authors: Zsolt Czekes[1,2*], Dóra Bai[1], Judit Vincze[1], Emese Gál[3], Zsuzsanna Nagy[1,4], Lucian Baia[2,5], Zsolt Pap[2,5,6*]

[1]Hungarian Department of Biology and Ecology, Babeș-Bolyai University, Cluj-Napoca, Romania

[2]Nanostructured Materials and Bio-Nano-Interfaces Center, Institute for Interdisciplinary Research on Bio-Nano-Sciences, Babeș – Bolyai University, Cluj-Napoca, Romania

[3]Faculty of Chemistry and Chemical Engineering, Babeș-Bolyai University, Cluj-Napoca, Romania

[4]Biological Research Centre, Institute of Biochemistry, MTA Lendület Laboratory of Cell Cycle Regulation, University of Szeged, Szeged, Hungary.

[5]Institute of Research-Development-Innovation in Applied Natural Sciences, "Babes-Bolyai" University, Cluj-Napoca, Romania

[6]Department of Applied and Environmental Chemistry, University of Szeged, Szeged, Hungary

Structural, morphological and optical analysis of P25 - instrumentation

X-ray diffraction (XRD) measurements were performed on a *Shimadzu 6000* diffractometer using Cu-Kα radiation (λ = 1.5406 Å), equipped with a graphite monochromator. The anatase - rutile phase ratio in P25 was evaluated using the Banfield' method [1], and the crystallites average size was calculated using the Scherrer equation [2].

JASCO-V650 spectrophotometer with an integration sphere (*ILV-724*) was used for measuring the *DRS spectra* of the samples (λ = 300-800 nm). To obtain the band-gap energy the reflectance data were converted to F(R) values according to the Kubelka-Munk theory [3]. The band gap was obtained from the plot of $[F(R)\cdot E]^{1/2}$ versus energy of the exciting light (E).

TEM images were obtained with a FEI Tecnai F20 field emission, high resolution Transmission Electron Microscope (TEM) operating at an accelerating voltage of 200 kV and equipped with Eagle 4k CCD camera.

Microprocessor controlled surface area analyzer, Qsurf Series M1, was used for the N_2 *adsorption measurements*. Outgassing at 200 °C was performed for 30 min, to ensure maximum

accuracy of the obtained information. The specific surface area of the samples was evaluated on the basis of Brunauer, Emmet and Teller (BET) equation.

A photoreactor system with three LighTech 40 W fluorescent lamps ($\lambda_{max} \approx 365$ nm, irradiation distance = 5 cm, irradiation time = 3 hours) was used to measure *the photocatalytic activities*. The photocatalyst suspension containing phenol (initial concentration of phenol $c_{0,\,phenol} = 0.5$ mM; catalyst concentration $c_{\,photocatalyst} = 1.0$ g/L; total volume of the suspension $V_{susp} = 50$ mL) was continuously purged by air in order to maintain the dissolved oxygen concentration constant during the whole experiment. The concentration decrease of the chosen organic substrate (phenol) and their degradation intermediates were followed using an *Agilent 1100 series HPLC* system.

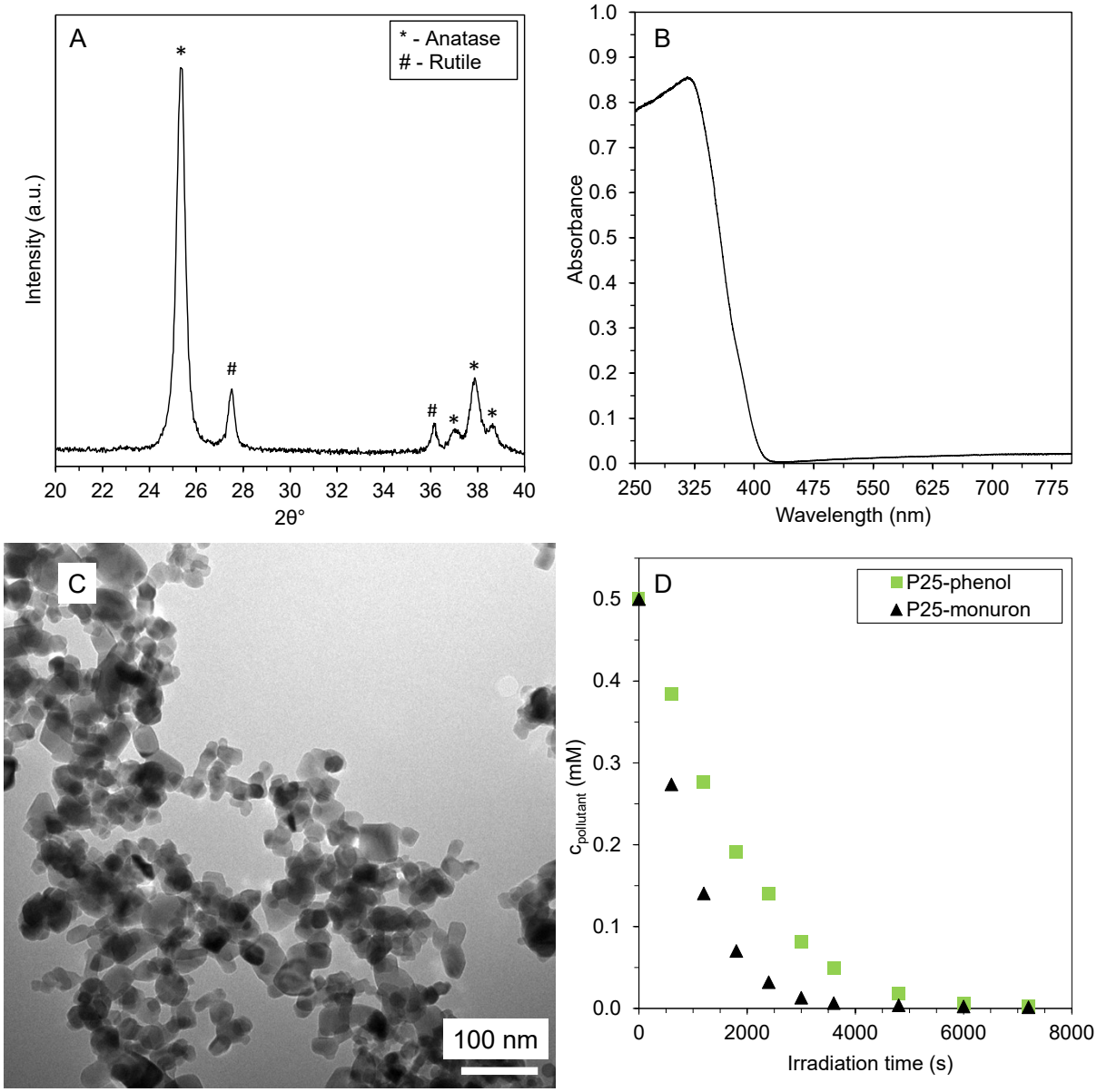

Figure S1. The XRD patterns of Evonik Aeroxide P25, showing, the specific signals for anatase and rutile, the first one being the main component (A), while the DRS spectrum of the material (B) demonstrates that the UV-A light is absorbed by the material, achieving the desired band-gap value). The size of the individual nanocrystals were ~25-40 nm (C) as seen in the TEM micrograph. The photoactivity was as expected from this material, as it removed in 2 hours both phenol and monuron (D) under UV-A irradiation.

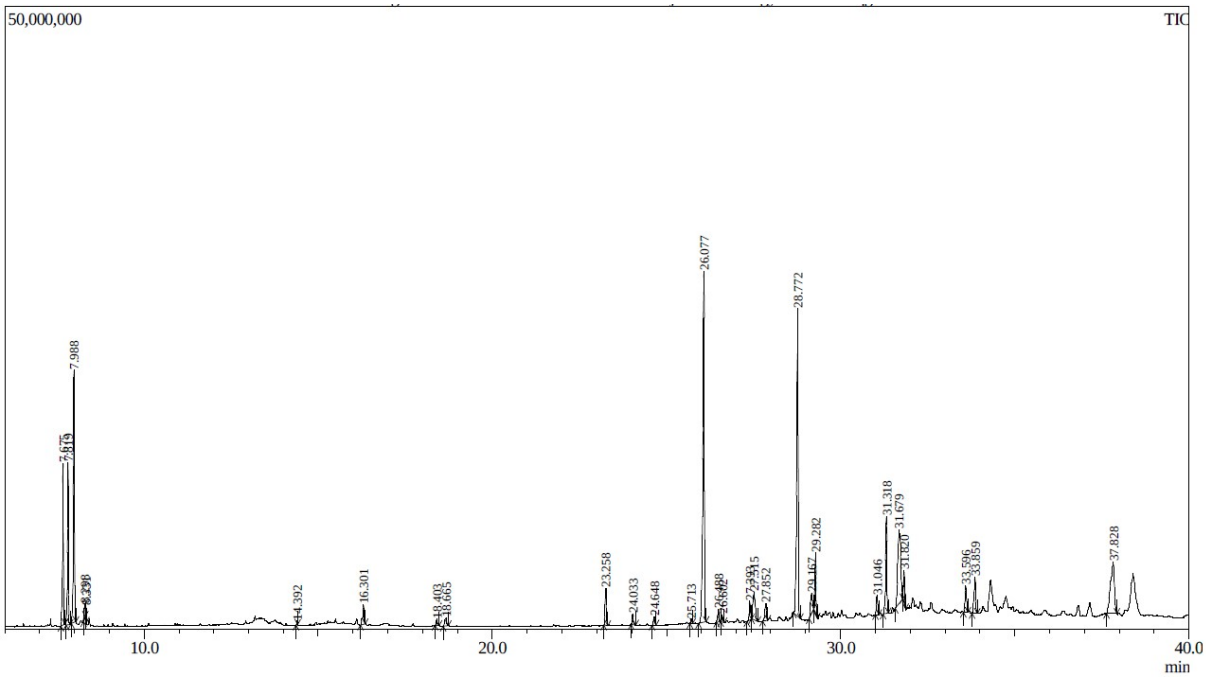

Peak#	R.Time	I.Time	F.Time	Area	Area%	Height	Height%	A/H	Mark	Name
1	7.675	7.605	7.730	23941373	5.68	12961308	8.67	1.85	MI	3-methyl heptane
2	7.819	7.755	7.875	24698146	5.86	13017820	8.71	1.90	MI	2,4-dimethyl-3-ethyl-pentane
3	7.988	7.915	8.040	39588663	9.39	20245232	13.55	1.96	MI	2,4-dimethyl-2-pentene
4	8.298	8.265	8.315	1978075	0.47	1133667	0.76	1.74	MI	E-4,4-dimethyl-2-pentene
5	8.331	8.315	8.350	1060810	0.25	1085578	0.73	0.98	MI	Z-4,4-dimethyl-2-pentene
6	14.392	14.365	14.415	436219	0.10	307693	0.21	1.42	MI	Myristic acid
7	16.301	16.220	16.350	4200803	1.00	1601969	1.07	2.62	MI	Palmitic acid
8	18.403	18.360	18.470	1067359	0.25	450837	0.30	2.37	MI	Oleic acid
9	18.665	18.585	18.740	2303515	0.55	620971	0.42	3.71	MI	Stearic acid
10	23.258	23.200	23.315	7312855	1.73	2988124	2.00	2.45	MI	Heneicosane
11	24.033	23.980	24.115	2282846	0.54	877465	0.59	2.60	MI	Phthalate-din extractie
12	24.648	24.590	24.705	1756360	0.42	665195	0.45	2.64	MI	Pentacosane
13	25.713	25.670	25.760	846746	0.20	343190	0.23	2.47	MI	Z-9-tricosene
14	26.077	25.925	26.140	84756266	20.11	28189611	18.87	3.01	MI	Heptacosane
15	26.488	26.440	26.555	2807204	0.67	983464	0.66	2.85	MI	Octacosane
16	26.602	26.560	26.655	1396357	0.33	596530	0.40	2.34	MI	9-buthyl-docosane
17	27.393	27.315	27.445	3624459	0.86	1507493	1.01	2.40	MI	Nonacosane
18	27.515	27.450	27.630	9351014	2.22	2183998	1.46	4.28	MI	Lonavar
19	27.852	27.765	27.910	4395124	1.04	1391363	0.93	3.16	MI	Squalene
20	28.772	28.655	28.845	73634916	17.47	24709735	16.54	2.98	MI	Hentriacontane
21	29.167	29.100	29.230	6595098	1.56	1643242	1.10	4.01	MI	Tetratriacontane
22	29.282	29.235	29.325	10965241	2.60	4891192	3.27	2.24	MI	Pentatriacontane
23	31.046	31.000	31.095	3840468	0.91	1526585	1.02	2.52	MI	17-Pentatriacontene
24	31.318	31.225	31.370	21848094	5.18	7772272	5.20	2.81	MI	Hexatriacontane
25	31.679	31.575	31.780	33290102	7.90	5935305	3.97	5.61	MI	Androstanazol
26	31.820	31.785	31.865	5573509	1.32	2615145	1.75	2.13	MI	M= 365
27	33.596	33.525	33.655	6036947	1.43	2162651	1.45	2.79	MI	Tritetracontane
28	33.859	33.770	33.920	10176746	2.41	2868280	1.92	3.55	MI	Tetratetracontane
29	37.828	37.635	37.935	31791820	7.54	4136656	2.77	7.69	MI	M= 491
				421557135	100.00	149412571	100.00			

Figure S2. The MS spectrum of CHC profile of *Formica Polyctena* before the interaction with the photocatalyst, showing 50x more intensive peaks than after the degradation process.

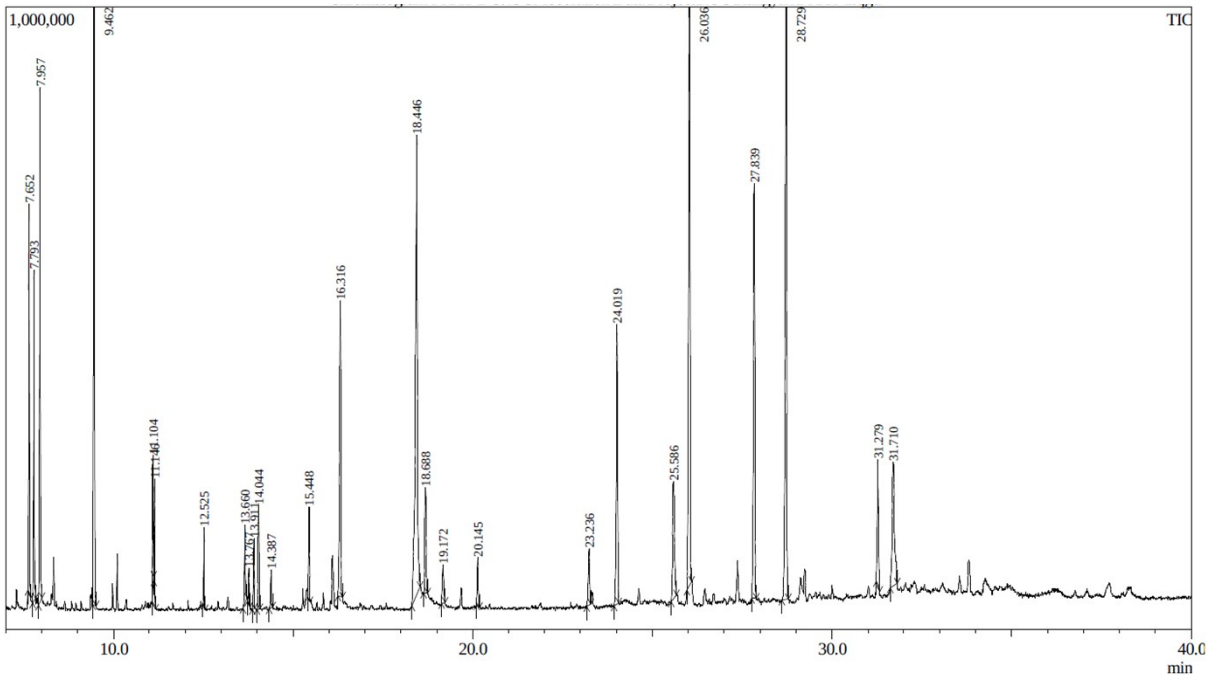

Peak#	R.Time	I.Time	F.Time	Area	Area%	Height	Height%	A/H	Mark	Name
1	7.652	7.620	7.700	951229	2.92	625903	3.45	1.52	MI	3-methyl-heptane
2	7.793	7.750	7.840	840401	2.58	531427	2.93	1.58	MI	2,4-dimethyl-3-ethyl-pentane
3	7.957	7.910	8.015	1311794	4.02	826194	4.55	1.59	MI	2,4-dimethyl-2-pentene
4	9.462	9.420	9.515	12243626	37.55	9479092	52.18	1.29	MI	Undecane
5	11.104	11.075	11.120	272004	0.83	208552	1.15	1.30	MI	5-tridecene
6	11.146	11.125	11.175	227946	0.70	182538	1.00	1.25	MI	Tridecane
7	12.525	12.490	12.560	172393	0.53	127503	0.70	1.35	MI	tetradecane
8	13.660	13.605	13.715	233266	0.72	125171	0.69	1.86	MI	E-7-tetradecan-1-ol
9	13.767	13.745	13.795	80170	0.25	57252	0.32	1.40	MI	4-decen-1-al
10	13.911	13.870	13.940	173164	0.53	113129	0.62	1.53	MI	Hexadecane
11	14.044	14.000	14.085	267101	0.82	166184	0.91	1.61	MI	Z-7-tetradecen -1-ol
12	14.387	14.340	14.440	107348	0.33	61245	0.34	1.75	MI	Myristic acid
13	15.448	15.410	15.480	240593	0.74	148676	0.82	1.62	MI	5-eicosene
14	16.316	16.250	16.375	1099080	3.37	474522	2.61	2.32	MI	palmitic acid
15	18.446	18.305	18.545	2788734	8.55	737939	4.06	3.78	MI	oleic acid
16	18.688	18.630	18.750	415756	1.28	170076	0.94	2.44	MI	Stearic acid
17	19.172	19.130	19.230	168610	0.52	61458	0.34	2.74	MI	E,E-farnesol
18	20.145	20.105	20.195	163470	0.50	77433	0.43	2.11	MI	1-Hexacosanol
19	23.236	23.170	23.295	223928	0.69	90053	0.50	2.49	MI	Heneicosane
20	24.019	23.930	24.070	1160437	3.56	449814	2.48	2.58	MI	Di-n-octhyl phthalate
21	25.586	25.530	25.670	662267	2.03	189022	1.04	3.50	MI	Z,E-Farnesol
22	26.036	25.960	26.095	2848772	8.74	1165214	6.41	2.44	MI	Heptacosane
23	27.839	27.765	27.895	1734819	5.32	666076	3.67	2.60	MI	squalene
24	28.729	28.615	28.785	2818578	8.65	1030812	5.67	2.73	MI	Hentriacontane
25	31.279	31.235	31.325	504383	1.55	203362	1.12	2.48	MI	Hexatriacontane
26	31.710	31.620	31.815	892705	2.74	198918	1.09	4.49	MI	M= 386
				32602574	100.00	18167565	100.00			

Figure S3. The MS spectrum of CHC profile of *Formica Polyctena* after the interaction with the photocatalyst, showing 50x more intensive peaks than after the degradation process.

References

1. Zhang, H. & Banfield, J. F. Understanding Polymorphic Phase Transformation Behavior during Growth of Nanocrystalline Aggregates: Insights from TiO_2. *The Journal of Physical Chemistry B* **104**, 3481–3487 (2000).

2. Jenkins, R. & Snyder, R. L. *Introduction to X-ray Powder Diffractometry*. *Chemical Analysis* (1996). doi:10.1002/9781118520994.

3. Kubelka, P. and Munk, F. Ein Beitrag Zur Optik Der Farbanstriche. *Zeitschrift für Technische Physik* **12**, 593–601 (1931).